The Impact and Causes of Subsidence in the Exmouth Sub-basin, Northern Carnarvon Basin

Patrick Makuluni
Minerals and Energy Resources
UNSW Sydney
Kensington, NSW
p.makuluni@unsw.edu.au

Stuart Clark
Mineral and Energy Resources
UNSW Sydney
Kensington, NSW
stuart.clark@unsw.edu.au

Juerg Hauser
Mineral Resources
CSIRO
Kensington, WA
juerg.hauser@csiro.au

SUMMARY

Understanding the kinematic processes around the formation of sedimentary basins is central to quantifying their resource potential. Building accurate kinematic models is a subjective and time-consuming process which requires incorporation of both vertical and lateral motions within sedimentary basins. Majority of plate reconstruction studies mostly focus on lateral plate motions hence, methods of subsidence analysis have seen slow evolution. So far subsidence analysis has been performed in one dimension only using borehole data and the results are interpolated or extrapolated over an area to give subsidence map of a region. This approach is prone to errors as it may not incorporate the effects of differential compaction within basins with complicated geology. We propose the introduction of an algorithm that performs decompaction and backstripping on 2D seismic cross-sections to improve the accuracy of subsidence analysis in the sedimentary basins. The decompaction component of the algorithm is based on the bisection method of a Python programming language. We applied the algorithm on an 87km wide seismic cross-section from the Exmouth Sub-basin of the Northern Carnarvon Basin in the Australian North West Shelf. The algorithm highlighted effects of differential compaction and quantified the spatial and temporal variability of subsidence within the area. One unique feature in the results is the variation of the basement morphology with time. This may be caused by faulting of the basement rocks from tectonic events and may also be due to the differential deflection of the basement from sediment loading. The tectonic subsidence periods coincide with the major tectonic events within the region as proposed by literature

Keywords: Subsidence analysis, decompaction, backstripping, Exmouth Sub-basin

INTRODUCTION

Vertical motion or subsidence is a vital component in the structural evolution of sedimentary basins, however, evidence shows that several tectonic reconstruction studies (i.e. Morgan, 1968) have focussed mostly on lateral plate motions. As suggested by Vibe et al. (2018), lack of direct link between plate margin tectonics and intraplate subsidence may be one of the reasons authors have struggled to understand the geodynamic mechanisms behind intraplate vertical motions. Despite lateral motions receiving more attention than vertical motions, there is an established history of authors' attempts to automate the subsidence history of sedimentary basins. Examples of such programs include; DEPOR and BURSUB (Stam et al., 1987), BASTA (Friedinger, 1988), BSAS (Jin, 1994), DeCompactionTool (Hölzel et al., 2008), BasinVis (Lee et al., 2016) and a recent algorithm by Said et al. (2015) which was also used by Vibe et al. (2018) to calculate subsidence history of the West Siberian Basin. These algorithms analyse the subsidence of single points and results from a few of these sparsely located points may further be interpolated over an area to give subsidence map of a region. This procedure may be prone to errors as it makes several assumptions and may not correctly incorporate effects of differential compaction within stratigraphic units. We introduce a program that can perform subsidence analysis on 2D seismic cross-sections using decompaction and backstripping algorithms. Thus, instead of data from a single point i.e. borehole, this program performs subsidence analysis of stratigraphic layers using data from multiple points along the span of a layer. There is no limit to the number of data points that the program can handle.

A decompaction technique aims at reversing the progressive effects of sediment compaction by restoring volume changes of rocks with time and depth (Allen and Allen, 1990). This technique is based on the porosity-depth law, equation (1) (Rubey and Hubbert, 1959) which assumes that the density changes in sedimentary units are caused only by changes in porosity (ϕ) which decreases exponentially with depth (y), in the equation (1), ϕ_0 is initial porosity. Backstripping is a technique that determines the quantity of tectonic subsidence by removing the effects of sediment load and sea level changes from the total subsidence (Allen and Allen, 2013), see equation 3 in the methods section.

$$\phi = \phi_0 e^{-cy} \quad (1)$$

We developed a decompaction and backstripping program in python and applied it on an interpreted 2D seismic cross-section from the Exmouth Sub-basin of the Northern Carnarvon Basin in the Australian North West Shelf. This paper presents the results of subsidence analysis of this region. It includes the timing, size, and causes of subsidence, and showcases the effects of differential compaction.

METHOD AND RESULTS

The decompaction function (equation 2) from Allen and Allen (2013) is non-linear and it can only be solved by numerical approximation (Allen and Allen, 1990). The aim is to compute the decompacted thickness of a stratigraphic layer given the present thickness, initial porosity, porosity coefficient and many other parameters as outlined in Table 1. From the equation, we have two unknowns; depths of the top and bottom levels of the decompacted layer and the pore space after decompaction. We employ the Bisection method in the

algorithm to calculate the unknowns in the equation. Python programming language has an in-build package of the Bisection method and further details about this method can be found in Kaw and Kalu (2009). We rearrange the decompaction equation into a real and continuous function to calculate the decompacted thicknesses at different depths and times.
The algorithm performs decompaction together with backstripping (equation 3) similar to the basic decompaction presented by Allen and Allen (2013), however, this time it has been applied on an interpreted 2D seismic cross-section.

$$y'_1 - y'_2 = (y_1 - y_2) - \frac{\phi_0}{c}\{e^{-cy_1} - e^{-cy_2}\} + \frac{\phi_0}{c}\{e^{-cy'_1} - e^{-cy'_2}\} \quad (2)$$

Table 1: Elements of the decompaction equation

Expression	Meaning (Allen and Allen, 1990)
$y'_1 - y'_2$	Decompacted thickness (new bottom – new top)
$(y_1 - y_2)$	Total thickness at the present (top and bottom depth at present)
$\frac{\phi_0}{c}\{e^{-cy_1} - e^{-cy_2}\}$	Pore space at present
$\frac{\phi_0}{c}\{e^{-cy'_1} - e^{-cy'_2}\}$	Pore space after decompaction

$$Y = S\left(\frac{p_m - \bar{p}_s}{p_m - p_w}\right) - \Delta_{SL}\left(\frac{p_w}{p_m - p_w}\right) + (w_d - \Delta_{SL}) \quad (3)$$

(Y is the basement depth in the absence of load, S is the sediment thickness, p_m, p_s, p_w are densities of the mantle, sediments and water respectively, w_d is water level and Δ_{SL} is sea level change)

The process begins from the onset of the basin formation, the algorithm removes all the layers and loads the bottom layer first followed by water-loading. The code computes the new thickness of the layer and the isostatic response due to this loading. The next step loads the second layer and compacts the bottom layer and repeat all the calculations until the final layer is added. The next stage computes subsidence and makes Palaeobathymetric and Eustatic corrections.

Data

We have applied the algorithm on an interpreted seismic cross-section from the Exmouth Sub-basin in the Northern Carnarvon basin of the North West Shelf Figure 1 (Geoscience Australia, 2018). The cross-section has 6 sedimentary layers.

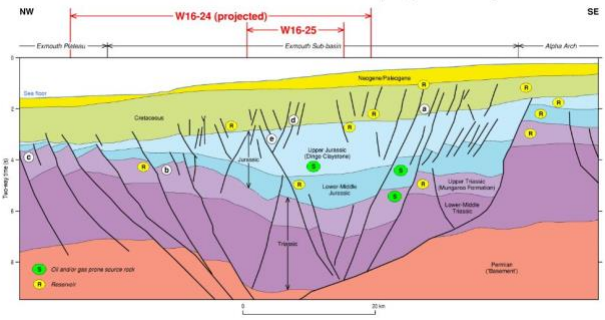

Figure 1: Interpreted seismic cross-section from Exmouth Sub-basin (Geoscience Australia, 2018)

We digitised the cross-section and converted the depth information from two-way time (seconds) to km using average speed of seismic waves in various lithologies multiplied by time, which gives layer thicknesses (Toksoz et al., 1976; Wanniarachchi et al., 2017). We then calculated the depth of the stratigraphic layer boundaries (Figure 1), followed by the collection of sedimentary layer features for example; lithology, absolute age, porosity, and many others as listed in Table 2, below. For every layer, we collected data from 48 uniformly distributed points along the span of the basin which is 87km long.

Table 2: Stratigraphic layer properties from the cross-section of Exmouth Sub-basin

Name and lithology	Absolute Age of deposition (Ma)	Surface porosity	Porosity coefficient (m^{-3})	Average density (kg/m^3)
Mungaroo Sandstone 1	238	0.49	0.27	2650
Mungaroo Sandstone 2	210	0.49	0.27	2650
Murat Siltstone	182	0.56	0.39	2460
Dingo Claystone	153	0.63	0.51	2720
Gearlie Siltstone	94	0.53	0.39	2460
Limestone	10	0.40	0.60	2560

Results

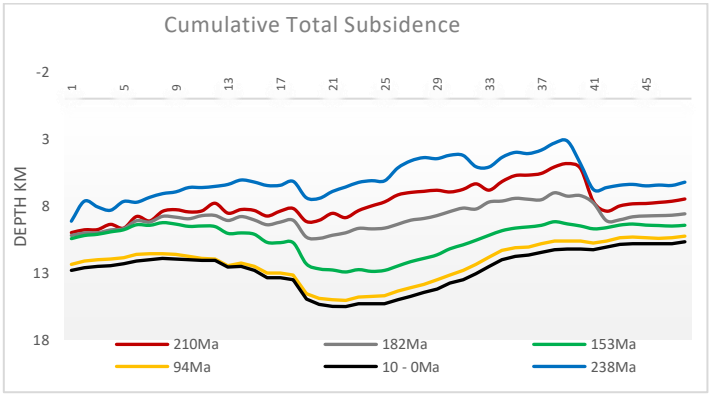

Figure 2: Total cumulative subsidence of the Exmouth sub-basin from Triassic to the present

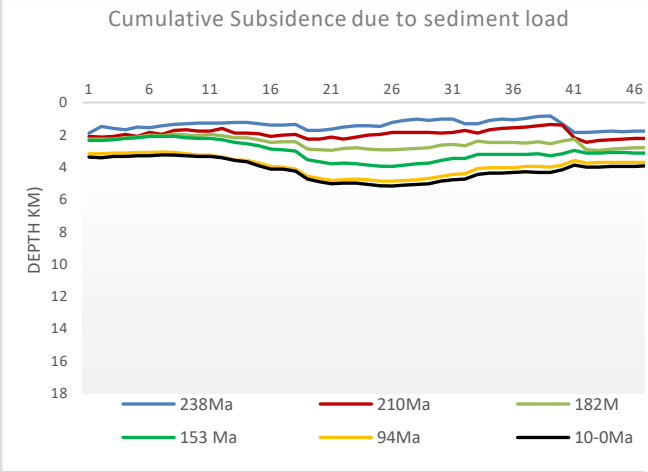

Figure 3: Cumulative subsidence due to sediment load in the Exmouth sub-basin from Triassic to the present

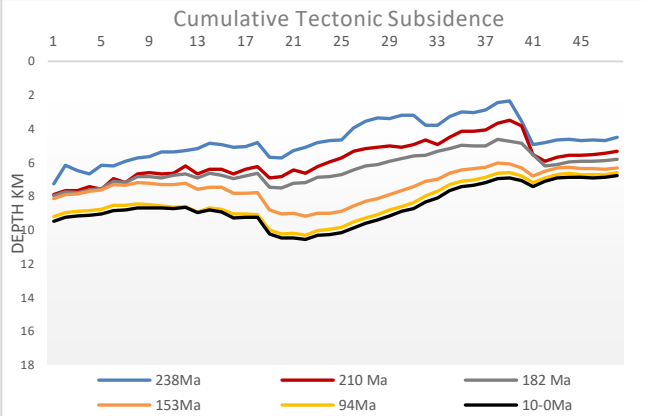

Figure 4*:* Cumulative tectonic subsidence of the Exmouth sub-basin from Triassic to the present

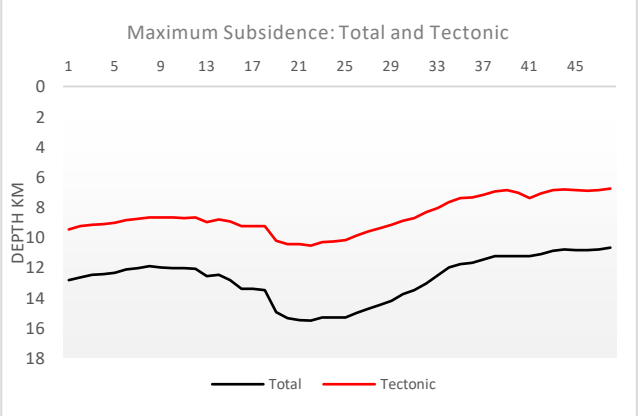

Figure 5: Total subsidence vs tectonic subsidence in the Exmouth Sub-basin.

Table 3 General statistics of tectonic subsidence in Exmouth sub-basin

Statistical measure	**300 - 238 Ma**	**238-210 Ma**	**210–182 Ma**	**182-153 Ma**	**153-94 Ma**	**94-10 Ma**
Mean (km)	**4.678**	**1.181**	**0.52**	**1.0458**	**0.92**	**0.248**
Maximum (km)	7.26	1.871	1.248	2.172	1.374	0.357
Minimum (km)	2.341	0.248	0.026	0.064	0.292	0.058
Standard deviation	1.1532	0.3297	0.349	0.7076	0.3398	0.0773
Count	48	48	48	48	48	48

Decompaction results

Results from the decompaction algorithm indicate that layers are progressively compacting with time from the time of basin inception, **Error! Reference source not found.** (appendix). Effects of differential compaction have been highlighted and schematically presented in **Error! Reference source not found.** (in the appendix). Thus, in Figure 7, a single layer displays spatial variability of compaction expressed as $\left\{\frac{\text{initial thickness} - \text{final thickness}}{\text{initial thickness}}\right\} \text{x } 100$. One striking feature in the results is the variation of the basement morphology with time **Error! Reference source not found.**. This may be due to faulting of the basement rocks from tectonic events and could also be due to the differential deflection of the basement from sediment loading as proposed by Allen and Allen (2013).

Subsidence results

Results from the backstripping algorithm are summarised in Figure 2, and they indicate the spatial and temporal variation of subsidence within the basin. They clearly indicate that the middle part, which is the depocenter of the basin, went through major tectonic subsidence as compared to the NW and SE margins/flanks of the basin. The absolute contribution of sediment load to subsidence is averagely uniform throughout the basin except between 210Ma to 153Ma, Figure 3. In this period, sediment load induced more subsidence within the middle section of the basin and along the SE flanks, however, it produced little to no subsidence in the NW flanks of the basin. Another notable result is that the 238 Ma Mungaroo sandstone and the 94 Ma Gearlie siltstone produced the largest subsidence throughout the basin compared to the rest of the sedimentary layers. After the deposition of the first sedimentary layer, the 238 Ma Mungaroo sandstone, most of the subsidence in the SE flanks of the basin were caused by sediment load. Tectonic events initially created around 6 km of accommodation space in the NW flanks of the basin compared to about 3km on the SE flanks Figure 4. The overall quantities of tectonic subsidence in the region compared to total subsidence is presented in Figure 5

Table 3 shows that major tectonic subsidence occurred during the inception of the Exmouth Sub-basin, with an average of 5.6 km deep and reaching maximum values of ~ 7km deep. Figure 4 displays the spatial variation of this tectonic subsidence along the span of the sub-basin. Authors have described this as the post-rift subsidence that followed the Permian extension within the region (Black et al., 2017). This was followed by another tectonic subsidence of ~1.18km deep on average and varying between 0.2 and 1.8km along the basin. This has been described as the tectonic subsidence that followed the Latest Triassic to Middle Jurassic extension (Longley et al., 2002). More details of the amount of tectonic subsidence in the region have been summarised in the Table 3 above.

Conclusions

We have developed an algorithm that can perform decompaction and backstripping of sedimentary basins using 2D seismic cross-sections. We have applied the algorithm to assess the timing, size, and causes of subsidence in the Exmouth Sub-basin. The algorithm has successfully quantified the temporal and spatial variability of compaction and subsidence in the sub-basin. Literature has described four major tectonic events in this region which coincide with the episodes of tectonic subsidence highlighted by our results. However, for the first time we have managed to quantify the subsidence caused by these tectonic events.

REFERENCES

Allen, A.., and Allen, R. (1990). Basin Analysis Principles and Applications (Blackwell Scientific Publications).

Allen, P., and Allen, J. (2013). Basin Analysis Principles and applications to Petroleum Systems (Wiley Blackwell).

Black, M., McCormack, K.D., Elders, C., and Robertson, D. (2017). Extensional fault evolution within the Exmouth Sub-basin, North West Shelf, Australia. Marine and Petroleum Geology *85*, 301–315.

Friedinger, P.J.J. (1988). BASTA—subsidence and paleotemperature modelling of rift basins. Computers & Geosciences. *14*, 505–526.

Geoscience Australia (2018). Map of Northern Carnarvon Basin.

Hölzel, M., Faber, R., and Wagreich, M. (2008). DeCompactionTool: Software for subsidence analysis including statistical error quantification. Computer Geoscience. *34*, 1454–1460.

Allen, A.., and Allen, R. (1990). Basin Analysis Principles and Applications (Blackwell Scientific Publications).

Allen, P., and Allen, J. (2013). Basin Analysis Principles and applications to Petroleum Systems (Wiley Blackwell).

Black, M., McCormack, K.D., Elders, C., and Robertson, D. (2017). Extensional fault evolution within the Exmouth Sub-basin, North West Shelf, Australia. Marine and Petroleum Geology *85*, 301–315.

Friedinger, P.J.J. (1988). BASTA—subsidence and paleotemperature modelling of rift basins. Computers & Geosciences. *14*, 505–526.

Geoscience Australia (2018). Map of Northern Carnarvon Basin.

Hölzel, M., Faber, R., and Wagreich, M. (2008). DeCompactionTool: Software for subsidence analysis including statistical error quantification. Computer Geoscience. *34*, 1454–1460.

Jin, J. (1994). BSAS: A basic program for two-dimensional subsidence analysis in sedimentary basins. Computer Geoscience. *20*, 1329–1345.

Kaw, A.., and Kalu, E.. (2009). NUMERICAL METHODS WITH APPLICATIONS (http://www.autarkaw.com).

Lee, E.Y., Novotny, J., and Wagreich, M. (2016). BasinVis 1.0: A MATLAB®-based program for sedimentary basin subsidence analysis and visualization. Computer Geoscience. *91*, 119–127.

Longley, L., Buessenschuett, L., Clydsdale, L., Cubitt, C., Davis, R., Johnson, M., Marshall, N., Somerville, R., and Spry, T. (2002). The North West Shelf of Australia Woodside perspective, The Sedimentary Basins of Western Australia 3: Proceedings of the Petroleum Exploration Society of Australia Symposium. PESA 27–88.

Morgan, W.J. (1968). Rises, trenches, great faults, and crustal blocks. Journal of Geophysics. Res. 1896-1977 *73*, 1959–1982.

Rubey, W.W., and Hubbert, M.K. (1959). Role of Fluid Pressure In Mechanics of Overthrust Faulting. Overthrust Belt In Geo-synclinal Area Of Western Wyoming In Light Of Fluid-Pressure Hypothesis. GSA Bulletin. *70*, 167–206.

Said, A., Moder, C., Clark, S., and Ghorbal, B. (2015). Cretaceous–Cenozoic sedimentary budgets of the Southern Mozambique Basin: Implications for uplift history of the South African Journal of African Earth Sciences 109, 1–10.

Stam, B., Gradstein, F.M., Lloyd, P., and Gillis, D. (1987). Algorithms for porosity and subsidence history. Computer Geoscience *13*, 317–349.

Toksoz, M.., Cheng, C.., and Timuri, A. (1976). Velocities of seismic waves in porous rocks. Geophysics *41*, 621–645.

Vibe, Y., Bunge, H.-P., and Clark, S.R. (2018). Anomalous subsidence history of the West Siberian Basin as an indicator for episodes of mantle induced dynamic topography. Gondwana Research. *53*, 99–109.

Wanniarachchi, W.A.M., Ranjith, P.G., Perera, M.S.A., Rathnaweera, T.D., Lyu, Q., and Mahanta, B. (2017). Assessment of dynamic material properties of intact rocks using seismic wave attenuation: an experimental study. Royal Society Open Science *4*.

Appendix

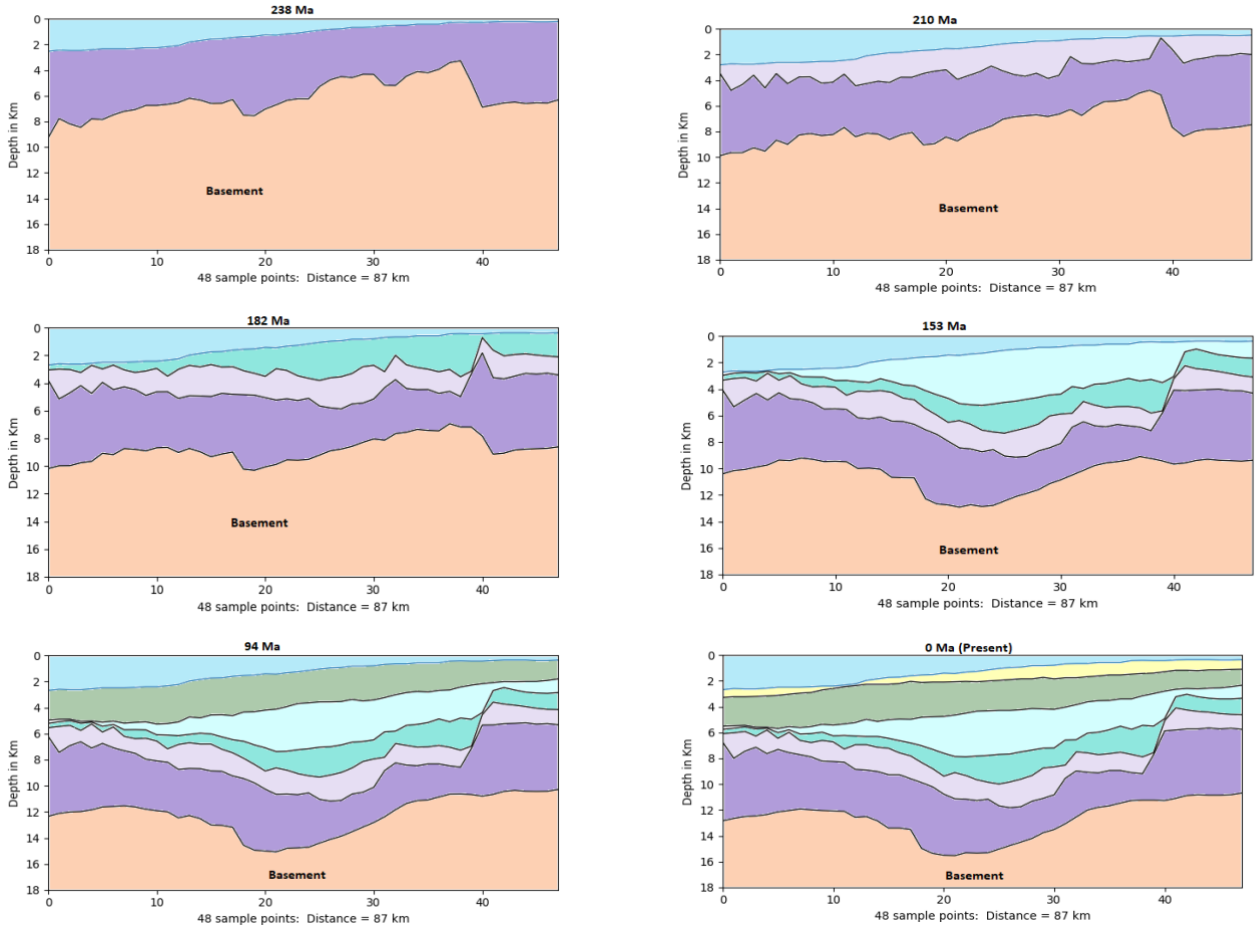

Figure 6: Decompaction results of Exmouth Sub-basin form 238 Ma to present

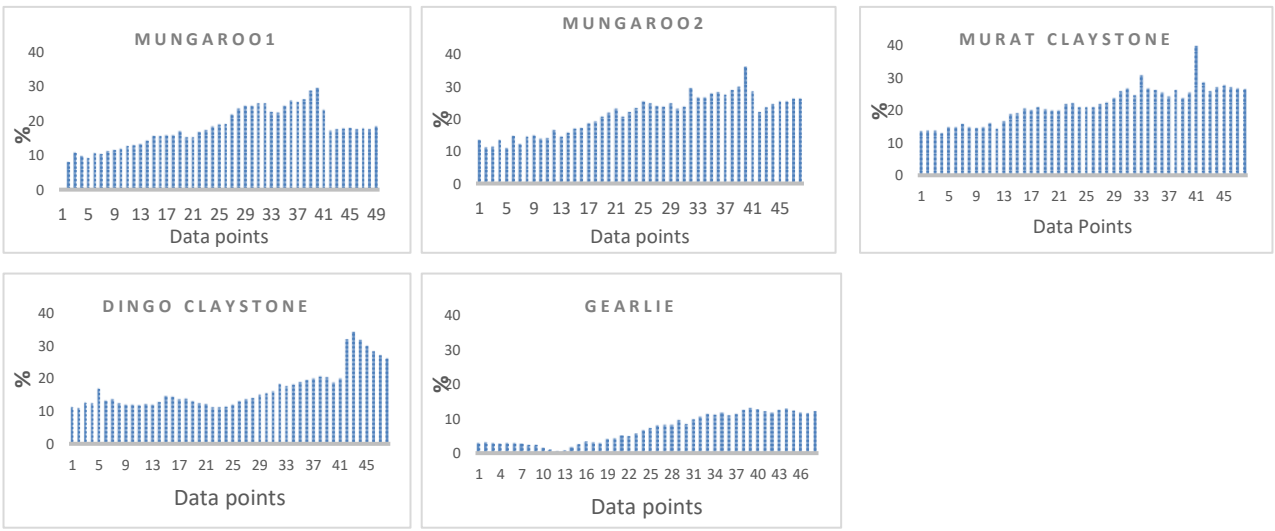

Figure 7: Differential compaction within respective sedimentary layers; expressed as $\left\{\frac{initial\ thickness - final\ thickness}{initial\ thickness}\right\} x100.$